Highly efficient terahertz detection by optical mixing in a GaAs photoconductor

Emilien Peytavit, F. Pavanello, Guillaume Ducournau, Jean-Francois Lampin

Highly efficient terahertz detection by optical mixing in a GaAs photoconductor

Cite as: Appl. Phys. Lett. **103**, 201107 (2013); https://doi.org/10.1063/1.4830360
Submitted: 30 September 2013 • Accepted: 28 October 2013 • Published Online: 12 November 2013

E. Peytavit, F. Pavanello, G. Ducournau, et al.

Highly efficient terahertz detection by optical mixing in a GaAs photoconductor

E. Peytavit,[a] F. Pavanello, G. Ducournau, and J.-F. Lampin
Institut d'Electronique, de Microélectronique et de Nanotechnologie, U.M.R C.N.R.S 8520, Université de Lille 1 Avenue Poincaré CS 60069, F-59652 Villeneuve d'Ascq Cedex, France

(Received 30 September 2013; accepted 28 October 2013; published online 12 November 2013)

It is shown from accurate on-wafer measurement that a low-temperature-grown GaAs photoconductor using a metallic mirror Fabry-Perot cavity can serve as highly efficient optoelectronic heterodyne mixer in the terahertz frequency range. Conversion losses of 22 dB at 100 GHz and ~27 dB at 300 GHz were measured, which is an improvement by a factor of about 40 dB as compared with the previous values obtained with photoconductors. Experimental results are interpreted satisfactorily by means of a simple electrical model of the optoelectronic mixing process. © *2013 AIP Publishing LLC*. [http://dx.doi.org/10.1063/1.4830360]

Sensitive and fast terahertz (THz) detectors are needed for various applications, such as gas spectroscopy, THz imaging, high data rate wireless communications, or characterization of high frequency electronic devices. At room temperature, the best performance in terms of sensitivity is obtained with electronic heterodyne mixers, commercially available for working frequencies reaching 1 THz. In return, unlike the direct detectors, such as low-barrier Schottky diodes, they need, in addition of a non linear device, a local oscillator that is not easily synthesized at THz frequencies. They are generally based on electronic frequency multiplier chains with poor wall plug efficiencies and narrow working frequency bands. An alternative way to this purely electronic solution is to use an optoelectronic mixer, in which the local oscillator is generated optically in a photodetector. In millimeter wave and THz technologies, ultrafast photodetectors are commonly used as photomixing sources.[1,2] The optical beatnote, produced by the spatial overlap of two slightly detuned (by a beating frequency f_B) infrared laser beams of same polarization, is indeed translated by the photodetector in a time varying carrier density and subsequently, in the presence of a constant electric field, in a conduction photocurrent having an oscillating term at f_B. The electric field can also have an oscillating term provided by an external radio-frequency (RF) source at a frequency f_{RF}, which generates mixing terms in the photocurrent flowing through the photodetector mainly at intermediate frequencies (IF) $f_{IF} = |f_{RF} \pm f_B|$. It forms a heterodyne mixer[3] with an optically generated local oscillator, which can therefore be used as the down converting part of an electromagnetic waves detector. Obviously, the efficiency of the mixing process is directly linked to the dependence of the photodetector's photocurrent on the bias voltage. Photoconductors, which can be modeled as linear photoconductances at low bias voltage, seem to be more suited than photodiodes which present photocurrents roughly independent on the bias voltage in standard experimental conditions.

In the THz range, the demonstration of homodyne detection (i.e., $f_B = f_{RF}$) with equivalent photoconductors and the same optical beatnote as the one used in emission[1,4] paved the way to commercial CW THz systems by avoiding helium cooled bolometer detection.[5] These first systems were based on 0.8-μm wavelength diode lasers and low-temperature-grown GaAs (LT-GaAs) ultrafast photoconductors. The LT-GaAs material is actually perfect for ultrafast optoelectronic devices because of its sub-picosecond carrier life-time and high dark resistance ($\rho_{dark} \approx 10^7$ Ω cm). This technology is still competitive regarding the signal to noise ratio (SNR) obtained, SNR ≈ 100 dB at $f_{RF} = 100$ GHz, compared with recently demonstrated systems using 1.5-μm-wavelength telecom lasers.[6]

In almost all these systems, the photoconductor used as detector consists of interdigitated electrodes capacitance patterned on a low-carrier lifetime photoconductive material. This planar electrodes device, which has its origin in the metal-semiconductor-metal (MSM) photodetector, is so far the most popular THz photoconductor used in emission as well as in detection, due to its simplicity of fabrication and its low electrical capacitance. Nevertheless, the performance of photoconductors based on the planar topology is quite low. It is indeed well established that output powers not greater than 10 μW have been generated in the millimeter wave and THz frequencies ranges by planar photomixers.[7] Used as detector, their performance have been assessed only through the SNR obtained in a complete system with no direct measurement of the conversion loss (L), which is one of the most relevant figures of merit in heterodyne detection. Nevertheless, it is possible to evaluate it roughly. In Ref. 5, a DC ($f_{IF} = 0$) detection current (I_d) of ~100 nA was measured at $f_{RF} = 100$ GHz using the previous presented scheme. For a 50-Ω load, the IF power is $P_{IF} = 50 \times I_d^2 = 0.5$ pW and the incident optical power is in the μW range, which gives a conversion loss $L = 10 \log(P_{RF}/P_{IF}) = 63$ dB. This is very high in comparison with narrow band electronic based mixer working in the same frequency range ($L \approx 10$ dB).

Recently, we have demonstrated by means of on-wafer measurements that up to 1.8 mW at 250 GHz (Ref. 8) could be generated by photomixing in a LT-GaAs vertical photoconductor pumped by 0.78-μm-wavelength lasers. This improvement, by a factor exceeding 100 in comparison with the previous state of the art, is obtained by means of a metallic mirror-based Fabry-Perot (FP) cavity and a deep submicron electrode spacing, which allow high carrier and current densities.[9,10] In this Letter, we investigate the performance of this

[a]Electronic mail: Emilien.peytavit@iemn.univ-lille1.fr

device as heterodyne mixer by means of on-wafer measurement at a frequency of 100 GHz and in the 220–325 GHz frequency range (called in the following J-band). In particular, we present accurate measurements of the conversion loss.

Fig. 1 shows a SEM micrograph of the photoconductor, consisting of a 0.16-μm-thick LT-GaAs layer sandwiched between two gold layers, which serve at the same time as bias electrodes and optical mirrors of the FP resonator. The 0.4-μm-thick buried gold layer is obtained thanks to the transfer of the LT-GaAs epitaxial layer onto a 2-in.-diameter silicon wafer.[11] The upper bias electrode consists of a 20-nm-thick semi-transparent gold layer and is linked by two air bridges to two 50-Ω thin film microstrip lines patterned on a 2.55-μm-thick-SiO_2 layer. The fabrication process of the LT-GaAs resonant photoconductor is detailed in Refs. 10 and 12. This structure can be considered similarly to a lossy FP resonator, which exhibits quantum efficiency peaks corresponding to the FP destructive interference condition, where $t_k \approx k \times \lambda/2 + \lambda/4$, with λ being the wavelength in the LT-GaAs. In this work, in order to enhance the photoconductor responsivity and the photoconductance while maintaining a sufficiently low capacitance per unit area, the first order peak was chosen (i.e., $k = 1$). Furthermore, the diameter of the resonant photoconductor is chosen to be 4 μm in order to minimize the capacitance.

A schematic overview of the photomixing experimental set-up is shown in Fig. 2. The optical beatnote is generated by spatially overlapping the emission of two fiber-coupled external cavity laser diodes (ECLD, New Focus Velocity TLB 6712-P), by means of a 50:50 polarization maintaining fiber coupler and used to seed a fiber-coupled tapered semiconductor optical amplifier (New Focus TA-7613). The wavelengths of the ECLDs are near 780 nm and are measured by a wavemeter with an 1-GHz-accuracy. The optical wave is then focused on the device by a lensed fiber providing a gaussian beam spot with a minimum width around 4 μm. At $f_{RF} = 100$ GHz, the signal is provided by a waveguide source based on a ×6 multiplier chain driven by a 0–20 GHz microwave synthesizer followed by a W-band power amplifier. A 75–110 GHz waveguide coplanar probe is used to transmit the signal to the LT-GaAs photodetector through the 50-Ω microstrip line. The available input power coupled to the latter is adjusted by means of a calibrated attenuator from −50 dBm to 10 dBm.

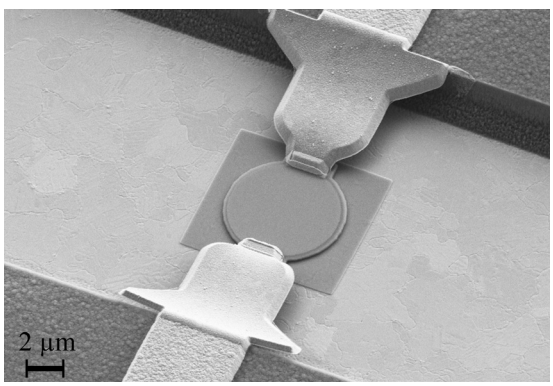

FIG. 1. SEM micrograph of a LT-GaAs metallic-mirror-based resonant photoconductor linked to two 50-Ω thin film microstrip lines.

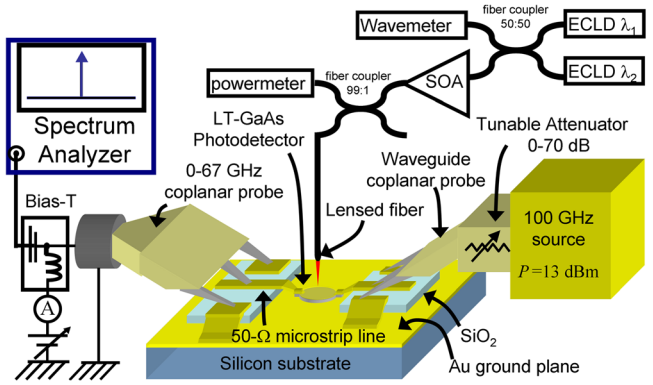

FIG. 2. Schematic of the on-wafer heterodyne detection experimental set-up: ECLD, external cavity laser diode; SOA, semiconductor optical amplifier.

In the higher band, the signal is provided by the source of a J-band frequency extender driven by a vector network analyzer (Rohde & Schwarz ZVA24). Its output power was measured by means of a powermeter (Erickson PM4) and is in the 1–20 μW range. In both cases, the mixing signal generated at a frequency f_{IF} is outcoupled by a 0–67 GHz coplanar probe and sent through a bias-T to a spectrum analyzer (SA). The measured power levels, P_{IF} and P_{RF}, are corrected for losses induced by the coplanar probes and by the waveguides. They reach 1.8 dB for the IF power, 1.2 dB for the RF power at 100 GHz, and ∼5 dB in the J-band. At each RF frequency, the wavelength of one of the two ECLD is tuned in order to have $f_{IF} \approx 400$ MHz.

In a first experiment, we measured the dependency of the conversion loss (L) on the bias voltage and on the optical power (P_{opt}). Fig. 3 shows the typical results obtained. For instance, at fixed optical power ($P_{opt} = +20.7$ dBm) and RF power ($P_{RF} = +2.7$ dBm), when the bias voltage is varied (Fig. 3(a)), the conversion loss reaches its minimum around $V_B = 0$ V. It corresponds to the minimum of the dc photoresistance (R_0), i.e., the inverse of the slope of the photocurrent-bias voltage curve ($R_0 = dV_B/dI_{dc}$) of the resonant photoconductor (inset of Fig. 3). R_0 would be constant if the tested device was a perfectly linear photoresistance. It should be noted that there is a slight dissymmetry of the curve with respect to the voltage polarity. It comes from the small variation of the photocarrier density along the LT-GaAs layer, which induces a low diffusion photocurrent. Fig. 3(b) shows the conversion loss as a function of the optical power (P_{opt}), illuminating the photoconductor for a RF power of +9.3 dBm and the optimum bias voltage $V_B \approx 0$ V. It is worth noting that the optical power range was limited in this work to the linear regime, in which R_0 is inversely proportional to the optical power, without any thermal saturation.[8] At low optical power, L decreases at the same rate as R_0^2 (plotted in Fig. 3(b)), following an inverse square law. Above 15 dBm of optical power occurs a saturation and L tends to ∼22 dB, whereas R_0 still decreases linearly.

In a second experiment, in order to evaluate the linear dynamic range of the mixer, we measured the IF power as a function of the 100 GHz RF Power (Fig. 4) for optimized values, i.e., $V_B \approx 0$ V and $P_{opt} = +20.7$ dBm. We obtained a constant conversion loss, of around 22 dB, for RF powers from about −50 dBm to +10 dBm. This is an improvement

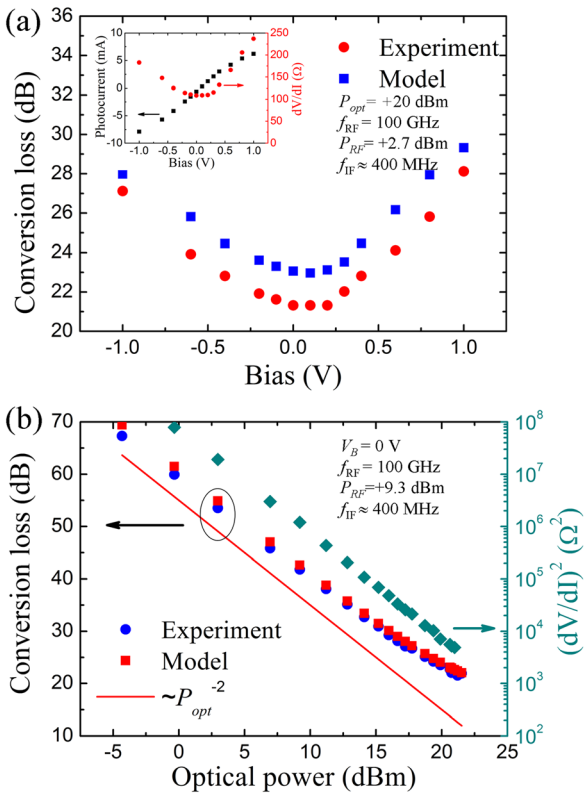

FIG. 3. Conversion loss as a function of (a) the bias voltage and (b) the optical pump power.

by 40 dB in comparison with the results achieved using a planar LT-GaAs photoconductor. As we will see later, the saturation of the IF power occurring at RF powers greater than +10 dBm can be mainly explained by the increase of R_0 at voltage greater than 0.5 V (see inset of Fig. 3(b)). A RF power $P_{RF} = +10$ dBm flowing through a 50-Ω-transmission line corresponds to a peak voltage $V_p = 1$ V, which is located in the non-linear part of the current-voltage characteristic.

Fig. 5 shows the spectrum of the IF signal obtained for 300 kHz of resolution bandwidth (RBW) (limited by the spectral stability of the ECLDs) and 15 dB of attenuation at the input of spectrum analyzer. It should be noted that the SNR is far from being optimized and is limited by the noise floor of

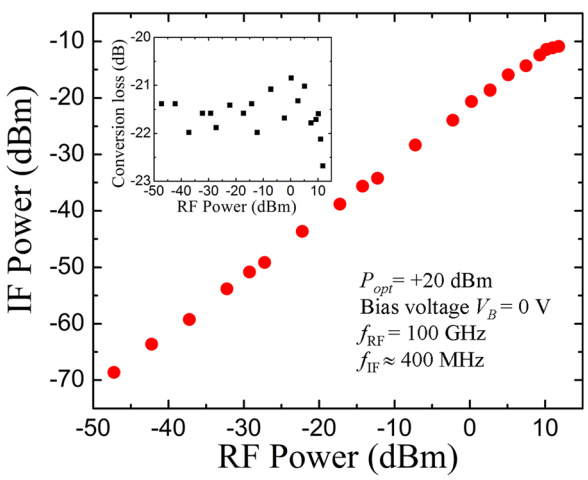

FIG. 4. Detected IF power as a function of the RF power. Inset: conversion loss dependency on the RF power.

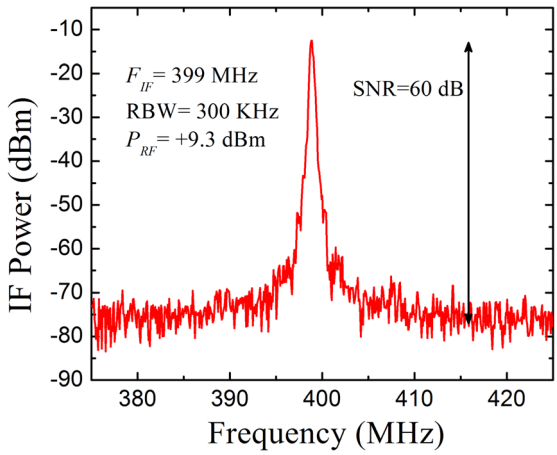

FIG. 5. IF Power frequency spectrum.

the spectrum analyzer and not by the optical mixer noise. This has been easily demonstrated by the verification of the independence of the noise floor on the dc photocurrent.

In order to show the ability of this device to work at higher frequencies, its conversion loss was measured on an other 4-μm-diameter device in the J-band with moderate RF power (~10 μW, depending on the frequency) at $V_B = 0$ V and $P_{opt} = +19.7$ dBm. A large ripple in the conversion loss plot can be seen in Fig. 6. In the J-band, it becomes difficult to have perfectly matched components, and the mismatches create reflected waves at each component interface. The photoconductor is then not loaded by constant impedances as the frequency varies, which can explain fluctuations of the conversion loss. However, the mean value seems to be constant around 27 dB, which is 4 dB higher than the $f_{RF} = 100$ GHz value.

These different experiments could be modeled thanks to the equivalent circuit given in Fig. 7, which is based on the work of Coleman and coworkers.[1] In this model, the photoconductor is modeled as a perfect time varying photoconductance $G(t) = G_0 + G_1 \cos(\omega_B t + \phi_B)$ shunted by an electrical capacitance C and followed by a serial resistance R_s. The ac photoconductance G_1 is proportional to the dc photoconductance G_0 with a frequency dependent proportionality factor: $G_1 = G_0(1 + \omega_B{}^2\tau^2)^{-1/2}$, where τ is the photocarrier lifetime in the LT-GaAs. The RF source is modeled as a time varying voltage source $V_{RF}(t) = V_{RF} \cos(\omega_{RF} t)$ of internal impedance $Z_s = 50$ Ω. The IF load Z_l is also assumed to be 50 Ω. Two ac

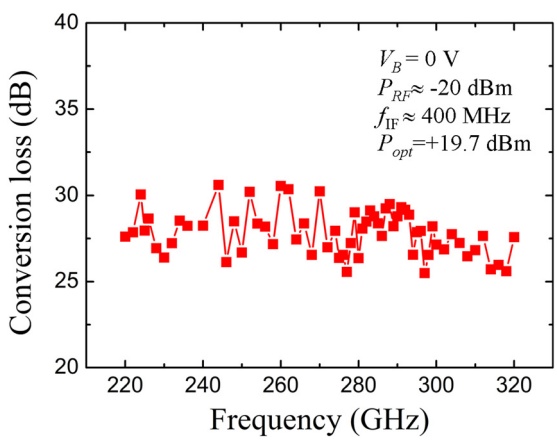

FIG. 6. Conversion loss as a function of the RF frequency in the J-band.

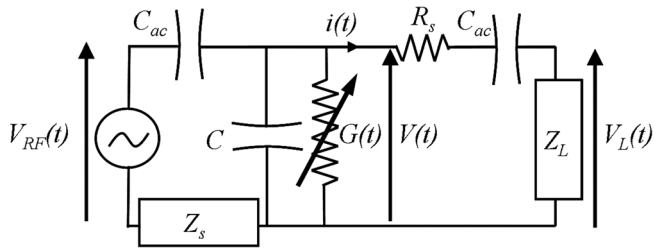

FIG. 7. Equivalent electrical circuit model. $V_{RF}(t) = V_{RF}\cos(\omega_{RF}\,t)$.

coupling capacitances C_{ac}, preventing from any dc current flowing in the circuit, but assumed to be large enough to behave as a short circuit at f_{IF} and f_{RF} are also added to model the Bias-T of the IF side and the intrinsic ac coupling of the waveguide coplanar probe.

As a first approximation, by neglecting all other mixing terms, we assume that the voltage $V(t)$ across the photoconductance has the simple form: $V(t) = V_{IF}\cos[\omega_{IF}t + \phi_{IF}] + V_0\cos[\omega_{RF}\,t + \phi_{RF}]$. Thus, in calculating the current $i(t) = G(t)V(t)$ and in resolving the loop equations at both frequencies, we obtain V_0 and V_{IF}. In the low RF frequency range, the effects due to the photoconductor capacitance and the photocarrier lifetime can be neglected. In this work, we evaluate from vector network analyzer (VNA) measurement a capacitance $C \approx 14$ fF. Furthermore, a photocarrier lifetime $\tau = 400$ fs was measured by time-resolved photoreflectance. Thus, at $f_{RF} = 100$ GHz, we can still neglect both effects. And by neglecting also R_s (evaluated to $\sim 5\ \Omega$ from the previous studies[8]), by assuming that $V_{IF} \ll V_0$ and by taking into account that $Z_s = Z_L$, the ratio V_{RF}/V_{IF} is of the simple form

$$\left|\frac{V_{RF}}{V_{IF}}\right| = \frac{2(2 + Z_L G_0)^2}{Z_L G_0}. \tag{1}$$

The RF power P_{RF} measured in this work is the available power from the voltage source of electromotive force V_{RF} and internal impedance Z_s, i.e., the dissipated power in a load $Z_L = Z_s$. Thus, $P_{RF} = {V_{RF}}^2/8Z_s$, and P_{IF}, the power dissipated in the load at f_{IF} is given by $P_{IF} = {V_{IF}}^2/2Z_L$. The conversion loss is then given by

$$L(dB) = 10\log\left(\frac{P_{RF}}{P_{IF}}\right) = 20\log\left(\frac{(2 + Z_L G_0)^2}{Z_L G_0}\right). \tag{2}$$

The above equation has a minimum equal to 18 dB reached at $Z_L G_0 = 2$, when the photoconductor impedance $(1/G_0)$ is matched to the resulting impedance Z of the source (Z_s) in parallel to the load (Z_L). Here, $Z_s = Z_L$ and $Z = Z_L/2$. The conversion loss has then a theoretical minimum $L = 18$ dB. It is worth mentioning that this simple result is valid only in the "small signal" regime in which the mixing term V_{IF} is much smaller than the RF term V_0. Furthermore, the photoconductor could be inserted in a microwave or THz circuit, classically used in electronic mixers, in which the IF power would be filtered on the RF side, and conversely the RF power would be filtered on the IF side. In this case, the minimum conversion loss would be $L = 12$ dB at $Z_L G_0 = 1$. The high conversion loss of the standard photoconductor (60 dB), even at low frequency is also easily explained by this basic model, since its very low photoconductance $(1/G_0 \sim 10\,\text{k}\Omega)$ is highly mismatched, at least with the internal impedance of the RF source given by the antenna impedance $(Z_L \sim 100\,\Omega)$. By assuming that $Z_L = Z_s = 100\,\Omega$, it gives $L = 52$ dB, which is close to the data extracted from the literature. On the contrary, in this work, the photoconductance is as low as $100\,\Omega$, which gives $L = 22$ dB, also very close to the experimental results. Fig. 3 shows the theoretical conversion loss at $f_{\text{RF}} = 100$ GHz using G_0 calculated from the slope of the experimental photocurrent-bias voltage curve. Here, we used a more complete model, frequency dependent, which takes into account the effects of the capacitance, the carrier lifetime, and the serial resistance. The slight discrepancy (<2 dB) between experimental and theoretical data can be explained by the difference between the effective impedance of the photoconductor and the one calculated from dc photocurrent-voltage curves. Measurements performed by means of a VNA up to 60 GHz show indeed that the small signal photoconductance is not constant at low frequencies, with a decrease by around 20% from dc to 20 GHz. This effect has a nanosecond time scale and is probably related to a charging effect in the LT-GaAs under illumination. Its study is however beyond the scope of this letter. Concerning the J-band experiment, the same model predicts a slight decrease of the conversion loss from $L \approx 25$ dB at $f_{\text{RF}} = 220$ GHz to $L \approx 27$ dB at $f_{\text{RF}} = 320$ GHz, with a 3-dB-cut off frequency $f_{3dB} = 260$ GHz. The discrepancy with the experimental data is higher than at $f_{RF} = 100$ GHz, which can be mainly explained by the uncertainty on the experimental source impedance and on the power measurements. From this model, we can expect $L \approx 40$ dB at $f_{\text{RF}} = 1$ THz and $L \approx 50$ dB at $f_{\text{RF}} = 2$ THz, values that seem still much lower than those that could be extracted from Ref. 5.

In conclusion, this work demonstrates that a LT-GaAs photoconductor can be used as a highly efficient THz heterodyne mixer with conversion losses much smaller than those obtained previously with optoelectronic devices. The addition of an appropriate circuit can further improve the performances. When compared with pure electronic solutions, the use of an optically generated local oscillator brings two main advantages: (1) an ultra wideband capabilities (>1:10) and (2) its easy transmission over long range by means of optical fibers.

[1]P. D. Coleman, R. C. Eden, and J. N. Weaver, IEEE Trans. Electron Devices **11**, 488 (1964).
[2]S. Preu, G. H. Döhler, S. Malzer, L. J. Wang, and A. C. Gossard, J. Appl. Phys. **109**, 061301 (2011).
[3]S. A. Maas, *Microwave Mixers* (Artech House Inc., 1986).
[4]S. Verghese, K. A. McIntosh, S. Calawa, W. F. Dinatale, E. K. Duerr, and K. A. Molvar, Appl. Phys. Lett. **73**, 3824 (1998).
[5]A. Roggenbuck, H. Schmitz, A. Deninger, I. C. Mayorga, J. Hemberger, R. Güsten, and M. Grüninger, New J. Phys. **12**, 043017 (2010).
[6]B. Sartorius, D. Stanze, T. Göbel, D. Schmidt, and M. Schell, Int. J. Infrared Millim. Terahz. Waves **33**, 405 (2012).
[7]J. E. Bjarnason, T. L. J. Chan, W. M. Lee, E. R. Brown, D. C. Driscoll, M. Hanson, C. Gossard, and R. E. Muller, Appl. Phys. Lett. **85**, 3983 (2004).
[8]E. Peytavit, P. Latzel, F. Pavanello, G. Ducournau, and J.-F. Lampin, IEEE Electron Device Lett. **34**, 1277 (2013).
[9]E. Peytavit, S. Lepilliet, F. Hindle, C. Coinon, T. Akalin, G. Ducournau, G. Mouret, and J.-F. Lampin, Appl. Phys. Lett. **99**, 223508 (2011).
[10]E. Peytavit, C. Coinon, and J.-F. Lampin, J. Appl. Phys. **109**, 016101 (2011).
[11]E. Peytavit, A. Beck, T. Akalin, J.-F. Lampin, F. Hindle, C. Yang, and G. Mouret, Appl. Phys. Lett. **93**, 111108 (2008).
[12]E. Peytavit, C. Coinon, and J.-F. Lampin, Appl. Phys. Express **4**, 104101 (2011).